

Chapter 2

Hierarchy of Terms in the Effective Hamiltonian

This lecture is an introduction to effective Hamiltonians, transition selection rules, Hund's coupling cases, pattern-forming rotational quantum numbers, and straight line plots. The goal is to create a fit model: \mathbf{H}^{eff} . This \mathbf{H}^{eff} must have the following desirable characteristics: (a) the \mathbf{H}^{eff} gives a good fit to both frequencies and relative intensities of measured transitions; (b) the \mathbf{H}^{eff} is capable of dealing with non-textbook spectra: perturbations [1], extra lines and intensity anomalies, for which there exist **no** directly applicable analytic formulas (Hund's cases); (c) the \mathbf{H}^{eff} permits reduction of spectra to "deperturbed" molecular constants, which provide a basis for extrapolation to other spectra, explanation of other anomalies (e.g. R , P intensity ratios in a fluorescence progression), and a compact, cause-and-effect generator of "dynamics". This is what I often refer to as going "Beyond Molecular Constants"; (d) the \mathbf{H}^{eff} provides a framework for comparison to theoretical calculations. Be careful, experimentalists and theorists often use the same name for different quantities (empirical fit vs. full deperturbation); and (e) there are three important terms in the \mathbf{H}^{eff} :

$$\mathbf{H}^{\text{eff}} = \mathbf{H}^{\text{electronic}}(R) + \mathbf{H}^{\text{spin-orbit}} + \mathbf{H}^{\text{rotation}}.$$

2.1 Adiabatic and Diabatic Representations

2.1.1 Introduction

There is no such thing as a textbook spectrum. In order to be able to make sense of a spectrum, one needs some simple ideas rather than a collection of all-purpose algebraic formulas. These ideas include *transition selection rules* and expected energy level patterns. An *effective Hamiltonian*, \mathbf{H}^{eff} , generates the energy level patterns [2]. One should never mistake the effective Hamiltonian for the exact

Hamiltonian. The \mathbf{H}^{eff} is much simpler and more useful. It forces the spectroscopist to make decisions about the expected relative magnitudes of the distinct physical effects represented by each of the additive terms in the Hamiltonian. The dreaded Hund’s coupling cases [3] arise from different orderings of the magnitudes of electronic, rotational, and spin–orbit terms. Hund’s cases are useful because they tell you what energy level pattern you should expect to find in the spectrum. Each Hund’s case corresponds to a different rotational pattern-forming quantum number and an explicit identification of a term that tries to disrupt that pattern.

Where do potential energy curves come from? What makes it possible to think of the solutions of the Schrödinger equation for a molecule as a product of an electronic wavefunction and a vibrational wavefunction? We label molecular energy levels with electronic and vibrational quantum numbers rather than some simple scheme in which the electronic-vibration eigenstates are numbered in energy order. The goal of this separation of molecular structure into electronic and vibrational parts is to enable insight, intuition, and simplification.

2.1.2 *Adiabatic vs. Diabatic Representations*

There are two quite different approaches to the electronic-vibrational structure of molecules: **adiabatic** and **diabatic** [4]. The former is mathematically rigorous and the latter is often more intuitively appealing. The one that a spectroscopist chooses to use to understand and represent a spectrum depends on the nature of the pathology expressed in the spectrum. When there is no pathology (the mythical textbook spectrum), the choice of adiabatic vs. diabatic approach is purely a matter of taste.

Because electrons “move much faster” than nuclei, it is reasonable to use the “clamped nuclei” = Born–Oppenheimer = adiabatic representation. At each nuclear geometry, we solve the electronic Schrödinger equation

$$\mathbf{H}^{\text{electronic}}(R) = \mathbf{H}^{\text{el}(0)}(R) + \sum_i \sum_{i < j} \frac{e^2}{4\pi\epsilon_0 r_{ij}(R)},$$

where geometry, R , is a parameter rather than a variable. The $1/r_{ij}$ term is segregated outside of $\mathbf{H}^{\text{el}(0)}$ because it contains, among many other important effects, the interactions between same-symmetry electronic states that are responsible for avoided crossings. This equation is solved on a grid of values of R . The solutions, $\psi_k^{\text{el}}(r; R)$, $E_k(R)$, are electronic wavefunctions that are functions of electron $\{r_i\}$ coordinates and parametrically dependent on nuclear coordinates $\{R_I\}$. We think of the $E_k(R)$ as a potential energy curve (diatomic molecules) or surface (polyatomic molecules) for the k -th electronic state. The vibrational wavefunctions, $\chi_v^k(R)$, and energy levels E_{v_k} are obtained by solving a nuclear motion Schrödinger equation for motion on the k -th potential energy surface, completely neglecting effects due to all other potential energy surfaces. This is a crucial approximation: the **Born–Oppenheimer** approximation [4].

For a diatomic molecule, adiabatic potential energy curves for electronic states of the same symmetry cannot cross [5]. They must avoid crossing. As a result, adiabatic curves often have peculiar shapes. This is a sign of something pathological. At an avoided crossing, the electronic wavefunction can change rapidly with internuclear distance, R . As a result, derivatives with respect to nuclear coordinates, R , of the $\psi_k^{\text{el}}(r; R)\chi_v^k(R)$ electronic-nuclear product wavefunction give rise to non-zero off-diagonal $k, v; k', v'$ matrix elements between different electronic-vibrational states. These inter-electronic state interactions, often called “kinetic energy couplings”, are caused by the neglected $\frac{\partial}{\partial R_I}$ and $\frac{\partial}{\partial R_I}\frac{\partial}{\partial R_J}$ terms operating on the electronic wavefunctions.

The idea that the electronic wavefunction might be strongly dependent on nuclear geometry offends intuition. A state is a state, or is it? The idea that electronic structure is roughly independent of nuclear geometry is embodied in the *diabatic* representation. Diabatic potential curves cross. They have “normal looking” shapes.

In the diabatic picture only part of \mathbf{H}^{el} is diagonalized. The part that is excluded is the part that causes avoided crossings. The big computational problem is that it is not possible to identify and isolate a particular term in \mathbf{H}^{el} that causes interactions between adiabatic electronic states of the same symmetry. The diabatic representation is intuitively appealing (a state is a state) but mathematically troublesome. If we had diabatic electronic states, $\{\psi_k^{\text{el, diab}}\}$, it would be possible to compute the set of vibrational wavefunctions and energy levels of each diabatic electronic state. But now inter-electronic interactions are neglected. It is necessary to add these interactions, in the form of factored interaction terms

$$\begin{aligned} H_{i v_i, j v_j}^{\text{el}} &= \langle \psi_i, v_i | \mathbf{H}^{\text{el}} | \psi_j, v_j \rangle \\ &= {}_r \langle \psi_i | \mathbf{H}^{\text{el}} | \psi_j \rangle_r {}_R \langle v_i | v_j \rangle_R \\ &= H_{ij}^{\text{el}} \langle v_i | v_j \rangle. \end{aligned}$$

It turns out, to a very good approximation, that

$$H_{ij}^{\text{el}} = \frac{\min [V_i^{\text{ad}}(R) - V_j^{\text{ad}}(R)]}{2}$$

(one-half the energy of closest approach of the two adiabatic curves) and the $H_{ij}^{\text{el}}(R)$ function is sampled at the R -value of this closest approach.

Whether the adiabatic or diabatic representation is more computationally convenient depends on the size of the would-be neglected interaction terms relative to the vibrational level spacings in the adiabatic or diabatic potential energy curves.

Whether one works in the adiabatic or diabatic representation, the key to getting started in modeling the energy levels observed in a spectrum is to obtain a complete electronic-vibrational basis set. In principle, we need

$$\{\psi_i^{\text{el}}(R)\}, \{E_i^{\text{el}}(R)\}, \{\chi_{v_i}(R)\}, \{E_{v_i}^{\text{vib}}\}$$

but in practice we need only a few $\psi_i^{\text{el}}(R)$ over a small range of R and only the $\chi_{v_i}, E_{v_i}^{\text{vib}}$ that are relevant to the region of the observed spectrum.

The selection rules for $\mathbf{H}^{\text{electronic}}$ are:

- $\Delta(\text{all angular momentum and symmetry quantum numbers}) = 0$
- $\langle \psi_i^{\text{el}} | \mathbf{H}^{\text{electronic}} | \psi_j^{\text{el}} \rangle = 0$ if ψ_i and ψ_j differ by more than two spin-orbitals.

A *spin-orbital* is a one-electron wavefunction that is labeled by body-frame orbital (λ) and spin (σ) quantum numbers: e.g. a p ($\ell = 1$) orbital gives six spin-orbitals: $1\alpha, 1\beta, -1\alpha, -1\beta, 0\alpha, 0\beta$.

For each $\Lambda - S$ electronic state (i) we get a potential energy curve, $V_{e_i}(R)$, either from theory or derived, via Rydberg-Klein-Rees (RKR-LeRoy), from experimental molecular constants [1, 6]. [See <http://leroy.uwaterloo.ca/programs.html> for RKR1 and LEVEL [7].] Every spectroscopist should know how to use these programs.

Input to RKR: two “dumb” power series:

$G(v)$ and $B(v)$ describe the v -dependence of vibrational energy levels

and rotational constants as power series in $v + 1/2$, where the coefficients

of each $(v + 1/2)^m [J(J + 1)]^n$ term are “Dunham constants.”

$$G(v) = \sum_{m=0}^{m_{\text{max}}} Y_{m0} (v + 1/2)^m \quad \{Y_{00}, \omega_e, \omega_e x_e, \omega_e y_e, \dots\}$$

$$B(v) = \sum_{m=0}^{m'_{\text{max}}} Y_{m1} (v + 1/2)^m \quad \{B_e, \alpha_e, \gamma_e, \dots\}$$

$$E_{vJ} = \sum_{m,n} Y_{mn} (v + 1/2)^m [J(J + 1)]^n \quad \text{Dunham expansion [8, 9].}$$

These are insight-free (dumb) representations of experimental data.

The Y_{mn} are dumb because they are a one-size-fits-all representation of experimental measurements. There is no intuitive or insightful model behind the Y_{mn} .

2.2 $\mathbf{H}^{\text{spin-orbit}}$ [10]

The spin-orbit term in \mathbf{H}^{eff} is widely misunderstood. Part of the mystery surrounding $\mathbf{H}^{\text{spin-orbit}}$ is due to its unnecessarily mysterious association with “relativistic” effects.

$$\mathbf{H}^{\text{spin-orbit}} = \sum_{i, \text{electrons}} a(r_i) \boldsymbol{\ell}_i \cdot \mathbf{s}_i \cong \mathbf{A} \mathbf{L} \cdot \mathbf{S} \quad (\text{a one-electron operator})$$

$a(r_i)$ is a radial function, $\sim 1/r_i^3$, heavily weighted in the near-nucleus region. The angular momentum operators, ℓ_i and s_i , are atomic one-electron operators, and are the primary reason for the simplicity and usefulness of the spin-orbit operator.

Matrix elements of \mathbf{H}^{SO} follow the rigorous selection rules:

$$\Delta\Lambda = 0, \pm 1$$

$$\Delta S = 0, \pm 1$$

$$\Delta\Sigma = -\Delta\Lambda$$

$$\Delta\Omega = 0$$

$$\Delta\text{parity} = 0$$

$$\Sigma^+ \leftrightarrow \Sigma^-$$

$$\Delta(\text{spin-orbitals}) = 0, \pm 1 \text{ (change in occupied spin-orbitals)}^\dagger$$

Λ is the projection of electronic orbital angular momentum on the internuclear axis. S is the total electron spin. Σ is the projection of \mathbf{S} on the internuclear axis. $\Omega = \Sigma + \Lambda$ is the projection of the total electron angular momentum (orbital and spin) onto the internuclear axis. Since the rotational angular momentum, \mathbf{R} , of a diatomic molecule is, by definition, perpendicular to the internuclear axis, Ω is also the projection of \mathbf{J} on the internuclear axis. The Σ^+ , Σ^- symmetry species expresses the effect of reflection (σ_v) of the electronic wavefunction for a Σ -state through a plane containing the inter-nuclear axis.

Note that the selection rules for the frequently used AL-S operator replacement for \mathbf{H}^{SO} are (misleadingly) more restrictive than those for the $a\ell_i \cdot s_i$ form of \mathbf{H}^{SO} .

The molecular spin-orbit interaction constant is closely related to atomic spin-orbit constants. It gets large for heavy atoms. It gets small as n^{*-3} , where n^* is the effective principal quantum number for Rydberg states.

$[IP - E_{n^*} \equiv \mathfrak{R}/n^{*2}]$ where \mathfrak{R} is the Rydberg constant, $109,737 \text{ cm}^{-1}$.

2.3 \mathbf{H}^{ROT} , the Rotational Operator [11]

\mathbf{H}^{ROT} contains the rotational angular momentum, \mathbf{R} , and an integral over the internuclear distance, R ,

$$\mathbf{H}^{\text{ROT}} = B_{ij}\mathbf{R}^2 = B_{ij}[\mathbf{J} - \mathbf{L} - \mathbf{S}]^2,$$

[†]If spin-orbitals are labeled 1, 2, 3, 4, ... then ψ_{1234} differs by one spin-orbital from ψ_{1235} or ψ_{1534} .

where B_{ij} is an integral of the “rotational constant” operator, $B(R)$, over the vibrational wavefunctions of the v_i and v_j states,

$$B_{ij} \equiv \frac{\hbar^2}{2\mu} \langle v_i | R^{-2} | v_j \rangle.$$

If the units of \mathbf{H}^{ROT} are energy (Joules), the units of B_{ij} are cm^{-1} , the angular momentum operator, \mathbf{R}^2/\hbar^2 , is converted into a unitless function of quantum numbers, then

$$B_{ij}/\text{cm}^{-1} = \frac{16.85762908}{\mu/\text{g} \cdot \text{mol}^{-1}} \langle v_i | R^{-2}/\text{\AA}^{-2} | v_j \rangle.$$

It is possible to arrange the angular momenta in several convenient ways. The one that I prefer is most appropriate for the Hund’s case (a) basis set, $|^{2S+1}\Lambda_\Omega\rangle = |n\Lambda S\Sigma\rangle |\Omega JM\rangle$ where $\Omega = \Lambda + \Sigma$.

$$\begin{aligned} \mathbf{R}^2 &= [\mathbf{J} - \mathbf{L} - \mathbf{S}]^2 = [\mathbf{J}^2 + \mathbf{L}^2 + \mathbf{S}^2 + 2\mathbf{L} \cdot \mathbf{S} - 2\mathbf{J} \cdot \mathbf{L} - 2\mathbf{J} \cdot \mathbf{S}] \\ &= [\mathbf{J}^2 - \mathbf{J}_z^2] + [\mathbf{L}^2 - \mathbf{L}_z^2] + [\mathbf{S}^2 - \mathbf{S}_z^2] \\ &\quad - [\mathbf{J}_+\mathbf{S}_- + \mathbf{J}_-\mathbf{S}_+] - [\mathbf{J}_+\mathbf{L}_- + \mathbf{J}_-\mathbf{L}_+] + [\mathbf{L}_+\mathbf{S}_- + \mathbf{L}_-\mathbf{S}_+] \\ &\qquad\qquad\qquad \text{S-uncoupling} \qquad\qquad \text{L-uncoupling} \qquad\qquad \text{orbit-spin}^\dagger \end{aligned}$$

The top line of the expression for \mathbf{R}^2 consists exclusively of terms that have diagonal matrix elements

$$\hbar^2 \{ [J(J+1) - \Omega^2] + L_\perp^2 + [S(S+1) - \Sigma^2] \}.$$

Because matrix elements of $\vec{\mathbf{L}}$ cannot be universally expressed for a non-spherical object, we replace the expectation value of $\mathbf{L}^2 - \mathbf{L}_z^2$ by the usually ignored fit-parameter, L_\perp^2 .

The second line of the expression for \mathbf{R}^2 consists of terms that have non-zero off-diagonal matrix elements between Hund’s case (a) basis functions. The $|^{2S+1}\Lambda_\Omega\rangle$ basis-functions are eigenfunctions of all of the operators in the first line.

2.4 Hund’s Cases[3]

Everyone except spectroscopists hates them. Spectroscopists need them because they tell what kind of patterns will be found among the energy levels. This enables spectra to be “assigned”. We are assured of being able to assign rigorously good

[†] *Orbit-spin* is not the same as *spin-orbit*.

quantum numbers (operators that commute with the exact \mathbf{H}), but the really difficult and important task is assignment of non-rigorously good quantum numbers. These non-rigorous quantum numbers are the basis for patterns in the spectrum that aid assignment of eigenstates and understanding of the dynamics encoded in these eigenstates.

There are three important terms in the molecular \mathbf{H}^{eff} .

1. \mathbf{H}^{el} (lifts the degeneracy of the states that arise from a single electronic configuration)
2. The spin-orbit term, \mathbf{H}^{SO} (diagonal in Ω), (lifts the degeneracy of the Ω -components of one $\Lambda - S$ state and mixes different $\Lambda - S$ states). For example, ${}^3\Pi$ is split into $\Omega = 0, 1, 2$ components and ${}^3\Pi_1$ can interact with ${}^1\Pi_1$.

$$E^{\text{SO}} = \langle n\Lambda S \Sigma | \mathbf{H}^{\text{SO}} | n\Lambda S \Sigma \rangle$$

$$\Omega = \Lambda + \Sigma$$

and

$$\langle n\Lambda = 1, S = 0, \Sigma = 0 | \mathbf{H}^{\text{SO}} | n'\Lambda = 1, S = 1, \Sigma = 0 \rangle \neq 0$$

3. \mathbf{H}^{ROT} (destroys Ω via the $B\mathbf{J}_{\pm}S_{\mp}$ and $B\mathbf{J}_{\pm}L_{\mp}$ spin- and L -uncoupling terms)

These three terms in the \mathbf{H}^{eff} are at war [12]. The relative orders of magnitude of differences between their expectation values guide us in the application of perturbation theory to this problem (see the discussion of perturbation theory in Chap. 3.1). They determine what we put into $\mathbf{H}^{(0)}$ and what acts as a perturbation and must be put into $\mathbf{H}^{(1)}$. We will see that this choice of how to partition \mathbf{H}^{eff} terms into $\mathbf{H}^{(0)}$ vs. $\mathbf{H}^{(1)}$ amounts to a choice of basis set.

- $\mathbf{H}^{(\text{el})} > \mathbf{H}^{(\text{SO})} > \mathbf{H}^{(\text{ROT})}$
 J is pattern-forming:
 Ω is good

$$\text{case (a)} \\ E(J) = \frac{B_{\Omega} J(J+1)}{B_{\Omega}} \text{ [the pattern is } J(J+1)\text{]} \\ B_{\Omega} = B + (B^2/A) \frac{2(\Omega-\Lambda)}{\Lambda}$$

- $\mathbf{H}^{(\text{SO})} > \mathbf{H}^{(\text{el})} > \mathbf{H}^{(\text{ROT})}$
 J is rotational pattern forming,

Ω is good. The atom-in-molecule quantum numbers $J_a = L_a + S_a$ might also be good. J_a is the total atomic angular momentum of one open-shell atom, appropriate for ligand field theory.

For example, in $\text{Ce}^{2+}\text{O}^{2-}$ the $\text{Ce}^{2+} f s$ configuration gives rise to $14 \times 2 = 28$ components: ${}^3\Phi$, ${}^1\Phi$, ${}^3\Delta$, ${}^1\Delta$, ${}^3\Pi$, ${}^1\Pi$, ${}^3\Sigma^+$, ${}^1\Sigma^+$.

These Λ - S state labels are the conventional but stupid way to look at the states and energy levels. Instead, f ($j = \frac{7}{2}$ and $\frac{5}{2}$) couples to s ($j = \frac{1}{2}$) to make $J_a = 4, 3, 3, 2$ components with the same energy level pattern as in a free Ce^{2+} atom [13] (see Fig. 2.1).

These four J_a atomic-ion components see the O^{2-} ligand as a point charge that splits each of them into $2J_a + 1$ components according to Ω_a , the projection of J_a on the internuclear axis. As a result, the pattern of four levels is replicated

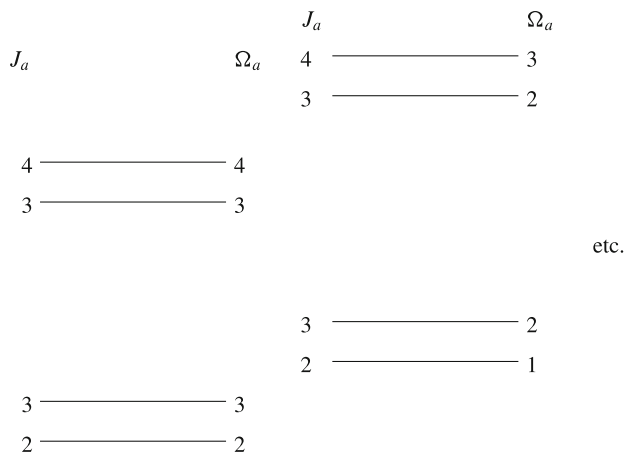


Fig. 2.1 The energy level pattern of four J_a atomic-ion components is replicated as \mathbf{J}_a goes from parallel to the internuclear axis ($\Omega_a = J_a$) toward perpendicular to the internuclear axis ($\Omega_a = 0$)

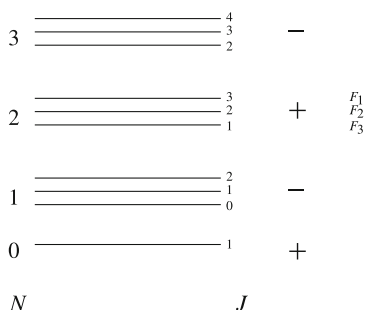


Fig. 2.2 The energy levels of a $^3\Sigma^+$ state. N is pattern-forming [$BN(N + 1)$] and the three J components of each N value exhibit a splitting pattern much smaller than $2BN$

and each replica is displaced by an energy related to the strength of the ligand field. This is an example of an unconventional energy level pattern that can be understood by choosing the physically appropriate basis set.

- $\mathbf{H}^{(el)} > \mathbf{H}^{(rot)} > \mathbf{H}^{(SO)}$ case (b)
 N^\dagger is rotational pattern-forming $E(N) = BN(N + 1)$
 Ω, Σ are not good. \mathbf{J} is good.

Σ -states are almost always in case (b) because their spin-orbit splitting is necessarily zero. The energy levels of a $^3\Sigma^+$ state are easy to understand when N is regarded as rotationally pattern forming (Fig. 2.2).

[†] N is the total angular momentum exclusive of spin, $\mathbf{N} = \mathbf{J} - \mathbf{S}$.

Consider $N = 2$. There are three spin components: $J = 1(F_3)$, $J = 2(F_2)$, and $J = 3(F_1)$. J can be rigorously determined via selection rules. If N is “good”, we can replace N in $BN(N + 1)$ by the appropriate value of J .

Rotational Energy

$$F_1 \ N = J - 1 \quad B(J - 1)(J) = B[J(J + 1) - 2J]$$

$$F_2 \ N = J \quad BJ(J + 1) = BJ(J + 1)$$

$$F_3 \ N = J + 1 \quad B(J + 1)(J + 2) = B[J(J + 1) + 2(J + 1)]$$

So if we make “reduced term value” plots of all rotational energy levels as $E(J) - BJ(J + 1)$ vs. J , we obtain three curves from which F_1, F_2, F_3 assignments, hence N assignments can be established by inspection.

- $\mathbf{H}^{(\text{rot})} > \mathbf{H}^{(\text{el})} > \mathbf{H}^{(\text{SO})}$ case (d)
 $R = N - \mathcal{L}$ is rotational pattern-forming,
 $E(R) = BR(R + 1) = B[N(N + 1) - 2\mathcal{L}N + \mathcal{L}^2 - \mathcal{L}]$.
 In the case (d) limit, a reduced term value plot of $E(N) - BN(N + 1)$ vs. N may be used to determine \mathcal{L} . \mathcal{L} is the projection of ℓ on \mathbf{R} .

Rydberg States. The Rydberg electron can be weakly coupled to the ion-core. When this occurs, the rotation-vibration levels of the ion-core form the dominant case (d) patterns that guide assignment of the spectra [14].

ℓ is good. \mathcal{L} , the projection of ℓ on \mathbf{R} (not on the z -axis!), is good.

- $\mathbf{H}^{(\text{SO})} > \mathbf{H}^{(\text{ROT})} > \mathbf{H}^{(\text{el})}$ case (e)
 Rydberg States $\left\{ \begin{array}{l} j \text{ is good (the total angular momentum} \\ \text{of the Rydberg electron)} \\ J^+ \text{ is good (the total angular momentum of the ion-core)} \end{array} \right.$
 J^+ is rotational pattern-forming ($\mathbf{J}^+ = \mathbf{J} - \mathbf{j}$). The pattern is $B^+ J^+(J^+ + 1)$.
 Usually a large $\mathbf{H}^{(\text{SO})}$ is associated with the ion-core, not with the Rydberg electron (the expectation value of $\mathbf{H}^{(\text{SO})}$ for the Rydberg electron scales as n^{*-3} , where n^* is the effective principal quantum number).
- $\mathbf{H}^{(\text{ROT})} > \mathbf{H}^{(\text{SO})} > \mathbf{H}^{(\text{el})}$ is usually ignored because it is impossible to make $\mathbf{H}^{(\text{el})}$ small while maintaining $\mathbf{H}^{(\text{SO})}$ as larger (except for Rydberg states built on an ion-core with a large, n^* -independent spin-orbit splitting), because both scale as n^{*-3} .
 (Hund's coupling cases correspond to these three terms arranged in $3! = 6$ orders.)

2.4.1 $\mathbf{H}^{(0)}$ vs. $\mathbf{H}^{(1)}$

Recall perturbation theory [15]: the energy of the n -th level is given by

$$E_n = E_n^{(0)} + E_n^{(1)} + E_n^{(2)} = H_{nn}^{(0)} + H_{nn}^{(1)} + \sum_m' \frac{|H_{nm}^{(1)}|^2}{E_n^{(0)} - E_m^{(0)}} \quad (' \text{ means } n \neq m)$$

Note that a large energy denominator keeps the basis set “good” but a large value of $|H_{nm}^{(1)}|$ makes the basis “bad”.

If $\mathbf{H}^{(\text{rot})}$ and $\mathbf{H}^{(\text{SO})}$ are at war, one choice of basis gives large energy denominators from $\mathbf{H}^{(\text{SO})}$ and small off-diagonal matrix elements as numerators from $\mathbf{H}^{(\text{ROT})}$. The other choice of basis gives large energy denominators from $\mathbf{H}^{(\text{ROT})}$ and small numerators from $\mathbf{H}^{(\text{SO})}$. One is free to chose either basis set, but the one for which the $\{E_n^{(0)}\}$ more closely resembles the observed pattern of eigen-energies is more convenient to use.

2.5 Two Basis Sets for the 2×2 “Two-Level” Problem

This example illustrates how the good and evil roles of opposing factors can be interchanged. Normally we think of zero-order energy level differences that appear along the diagonal of an \mathbf{H}^{eff} , such as the spin-orbit $A\Lambda\Sigma$ term, as good because they preserve the simple case (a) level pattern. The non-diagonal $-BJ_{\pm}L_{\mp}$ L -uncoupling term is evil because, at sufficiently high- J [$J > \frac{A\Lambda}{B}$] it vanquishes $A\Lambda\Sigma$ and forces the level pattern to follow case (d). In case (d), what remains of the influence of \mathbf{H}^{SO} resides off-diagonal between same- J , same-parity, different- N basis states. The simplest illustration of this role-reversal between \mathbf{H}^{SO} and \mathbf{H}^{ROT} is the two-level problem.

The $\mathbf{H}^{(\text{eff})}$ for the 2×2 problem is usually expressed as

$$\begin{aligned} E_1^{(0)} &= \bar{E} + \Delta/2 & \bar{E} &= \frac{E_1^{(0)} + E_2^{(0)}}{2} \\ E_2^{(0)} &= \bar{E} - \Delta/2 & \Delta &= E_1^{(0)} - E_2^{(0)} \\ \mathbf{H}_{12}^{(1)} &= \langle 1 | \mathbf{H}^{(1)} | 2 \rangle = V_{12} \\ \mathbf{H} &= \begin{pmatrix} \bar{E} & 0 \\ 0 & \bar{E} \end{pmatrix} + \begin{pmatrix} \Delta/2 & V_{12} \\ V_{12} & -\Delta/2 \end{pmatrix}. \end{aligned}$$

The Δ term tries to keep the basis “good” and the V_{12} term opposes Δ . The eigenvalues are $E_{\pm} = \bar{E} \pm [(\Delta/2)^2 + V_{12}^2]^{1/2}$. This basis is more convenient when

$|\Delta| \gg |V_{12}|$. Now consider a change of basis set:

$$|a\rangle = 2^{-1/2}[|1\rangle + |2\rangle]$$

$$|b\rangle = 2^{-1/2}[|1\rangle - |2\rangle]$$

$$\langle a|\mathbf{H}|a\rangle = \frac{1}{2}[H_{11} + H_{22} + 2V_{12}] = \bar{E} + V_{12}$$

$$\langle b|\mathbf{H}|b\rangle = \frac{1}{2}[H_{11} + H_{22} - 2V_{12}] = \bar{E} - V_{12}$$

$$\langle a|\mathbf{H}|b\rangle = \langle b|\mathbf{H}|a\rangle = \frac{1}{2}[H_{11} - H_{22} + V_{12} - V_{12}] = \Delta/2$$

The transformed $\mathbf{H}^{(\text{eff})}$ is

$$\tilde{\mathbf{H}} = \begin{pmatrix} \bar{E} & 0 \\ 0 & \bar{E} \end{pmatrix} + \begin{pmatrix} V_{12} & \Delta/2 \\ \Delta/2 & -V_{12} \end{pmatrix}$$

The V_{12} term tries to keep the basis good while the Δ term opposes V_{12} . This basis is more convenient when $|V_{12}| \gg |\Delta|$. Notice that $\Delta/2$ and V_{12} have exchanged roles [16]!

2.6 Some Reasons for Patterns

It is usually clear in advance which Hund's case will be most appropriate (because we know how $\mathbf{H}^{(\text{SO})}$ and $\mathbf{H}^{(\text{el})}$ scale with n^{*-3}).

Σ -states are always case (b) except at lowest N . Why? [The spin-spin term lifts the degeneracy of same- J , different- Ω states.] There is no force that tells \mathbf{S} the location of the body axis. Each N is $2S + 1$ degenerate: the fine structure components $J = N - S$ (F_{2S+1}) to $N + S$ (F_1) and all $2S + 1$ spin-components have the same total parity, which is $(-1)^N$ for Σ^+ states and $(-1)^{N+1}$ for Σ^- states. (F_i is a special notation for the labeling of spin components [17].) J and parity are always good.

Rydberg states generally have two flavors:

1. *core-non-penetrating*, ℓ is good because the Rydberg electron is a passive passerger, thus ion-core quantum numbers are pattern-forming;
2. *core-penetrating*, ℓ is bad, ℓ and s couple to the ion-core quantum numbers to make N and J . For example Rydberg states of the HfF molecule have half-integer rotational pattern-forming quantum numbers (even though ion-core is $^1\Sigma^+$) [18]. The half-integer quantum numbers imply that the Rydberg electron still has strong enough $\mathbf{H}^{(\text{SO})}$ that $\mathbf{H}^{(\text{SO})} > \mathbf{H}^{(\text{rot})}$.

2.7 Straight Line Plots

Consider a ${}^2\Pi$ state. It is really four states (${}^2\Pi_{3/2e}$, ${}^2\Pi_{3/2f}$, ${}^2\Pi_{1/2e}$, ${}^2\Pi_{1/2f}$), treated as one. Will the pattern-forming rotational quantum number be integer or half integer?

case (a)	case (b)
J , half integer	N , integer
$E(1/2) = \frac{3}{4}B$	$E(0) = 0B$
$E(3/2) = \frac{15}{4}B$	$E(1) = 2B$
$E(5/2) = \frac{35}{4}B$	$E(2) = 6B$

$\left. \begin{array}{l} \\ \\ \end{array} \right\} 3B$
 $\left. \begin{array}{l} \\ \\ \end{array} \right\} 5B$

$\left. \begin{array}{l} \\ \\ \end{array} \right\} 2B$
 $\left. \begin{array}{l} \\ \\ \end{array} \right\} 4B$

The consecutive level spacing pattern $3B, 5B, \dots$ (energy levels linear in $J(J + 1)$) is easily distinguished from $2B, 4B, 6B, \dots$ (energy levels linear in $N(N + 1)$).

Consider a case (b) ${}^3\Sigma^+$ State (no spin-orbit)

parity $(-1)^N$

J is rigorously good (revealed by selection rules) but N is pattern-forming (revealed by pattern).

$$\begin{aligned} J = N + 1 &\text{ goes as } B(J - 1)J && F_1 \\ J = N &\text{ goes as } BJ(J + 1) && F_2 \\ J = N - 1 &\text{ goes as } B(J + 1)(J + 2) && F_3 \end{aligned}$$

From a “stacked plot” of spectra recorded by excitation from consecutive J'' values [14], we know J . So we can make a *reduced term value plot* that displays the correct value of N . The reduced term value is [19]

$$\begin{aligned} E(J) - \bar{B}J(J + 1) &= -2\bar{B}J = -2\bar{B}(N + 1) && F_1 \\ E(J) - \bar{B}J(J + 1) &= 0 && F_2 \\ E(J) - \bar{B}J(J + 1) &= 2\bar{B}(J + 1) = 2\bar{B}N. && F_3 \end{aligned}$$

When we plot the reduced term values of a ${}^3\Sigma^+$ state vs. J [not $J(J + 1)$ nor N nor $N(N + 1)$!], we get three straight-line plots with slopes $-2\bar{B}$, 0 , and $+2\bar{B}$. These patterns enable assignment of N (Fig. 2.3).

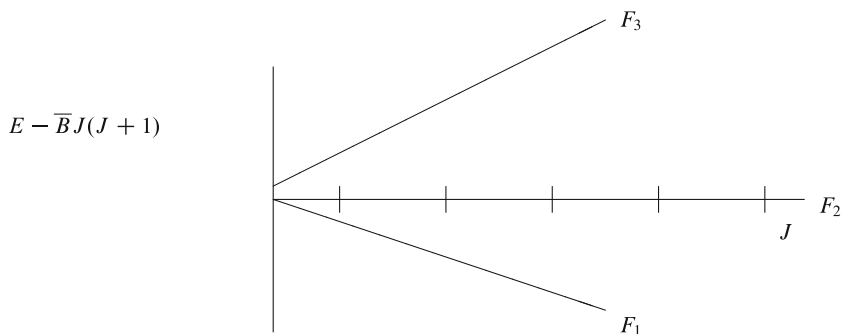


Fig. 2.3 A reduced term value plot of $E(J) - BJ(J + 1)$ vs. J for a $3^3\Sigma^+$ state in case (b). J is always a rigorously good quantum number, so J can always be determined from the spectrum. The reduced term value plot is based on known quantities $E(J)$ and J and is used to determine a non-rigorously good but pattern-forming quantum number, N

2.8 Stacked Plots

What is the difference between rigorous and pattern-forming quantum numbers? A rigorous quantum number is related to the eigenvalue of an operator that commutes with the exact molecular Hamiltonian, for example J (\mathbf{J}^2) and parity \pm are rigorously good quantum numbers for an isolated molecule at zero external magnetic and electric fields. It is always possible (but not always trivial) to determine the *rigorously good quantum numbers* of every eigenstate. Methods include Optical Optical Double Resonance (OODR) via a J - and parity-assigned intermediate state. From each J , + intermediate state, the second transition can only terminate in $(J - 1)$ -, J -, and $(J + 1)$ -final states. J -assignments are secured via lower-state rotational combination differences, as illustrated by Fig. 2.4, or by polarization diagnostics [20].

Complete specification of an eigenstate often requires the use of *approximately good quantum numbers* as labels in addition to the rigorously good quantum numbers, as illustrated in Figs. 2.5 and 2.6.

These additional labels are often eigenvalues of an operator that does not commute with the exact Hamiltonian, for example $\mathbf{N} = \mathbf{J} - \mathbf{S}$. However, in the limit that some term in the exact Hamiltonian can be neglected (e.g. the effects of \mathbf{H}^{SO} can be negligible at high- J relative to the effects of the $-B\mathbf{J} \cdot \mathbf{S}$ spin-uncoupling term from \mathbf{H}^{ROT}). When this occurs, N (\mathbf{N}^2) becomes pattern-forming, and it is possible to use the $BN(N + 1)$ pattern in the spectrum to determine the value of the N quantum number. At high enough J , N becomes pattern-forming

$$\bar{B}N(N + 1) = \bar{B}(J - S)(J - S)(J - S + 1) = \bar{B}[J(J + 1) - 2JS + S^2 - S]$$

where $S \equiv J - N$, S changes in steps of 1 in the interval, $[-S \leq S \leq S]$ and is the projection of \mathbf{S} on \mathbf{N} . \bar{B} is the approximately known rotational constant (for Rydberg

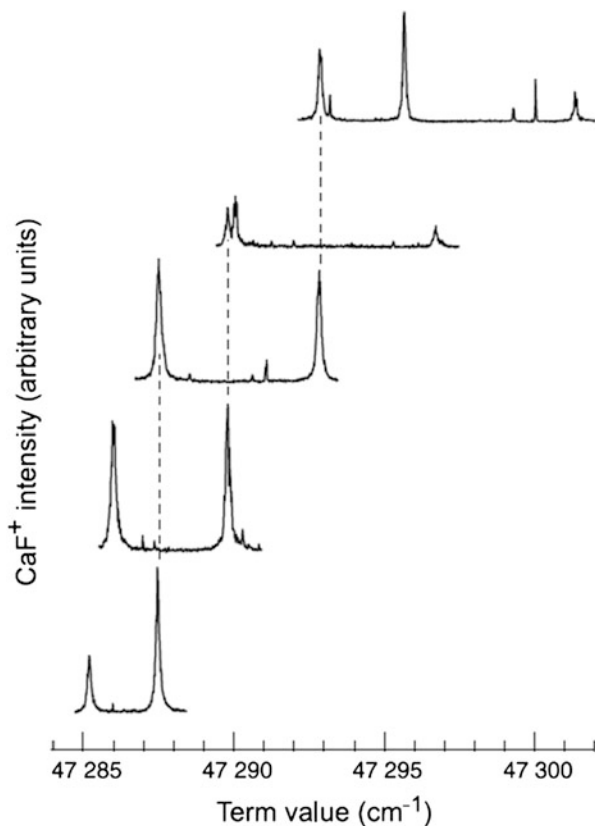


Fig. 2.4 Term value stacked plot. A consecutive- N' series of optical-optical double resonance spectra [Rydberg $\leftarrow D^2\Sigma^+$, $D^2\Sigma^+ \leftarrow X^2\Sigma^+$] of CaF is plotted vs. the absolute energy of the upper Rydberg level. Each Rydberg $\leftarrow D^2\Sigma^+$ spectrum is shifted by the absolutely known term value of the intermediate N' level, which is the term value of the $X(v'', N')$ initial level plus the transition frequency of the laser that pumps the D - X transition. Transitions connected by a vertical dashed line terminate in the same upper N -level. The value of this N quantum number is determined by the D -state rotational combination difference, $R(N-1) - P(N+1)$ [14]. Reproduced with permission from Fig. 4 in J.J. Kay, D.S. Byun, J.O. Clevenger, V.S. Petrovic, R. Seiler, J.R. Barchi, A.J. Merer, and R.W. Field, *Can. J. Chem.* **82**, 791–803 (2004). Copyright 2004, Canadian Science Publishing or its licensors

states it is the rotational constant of the molecular ion-core, for triplet states it is the effective rotational constant of the F_2 ($J = N$) spin-component. A reduced term value plot of

$$E^{\text{ROT}}(J) - \bar{B}J(J+1) = \bar{B}[-2JS + S^2 - S] \text{ vs. } J$$

has slope $-2\bar{B}S$, from which S and then N are determined.

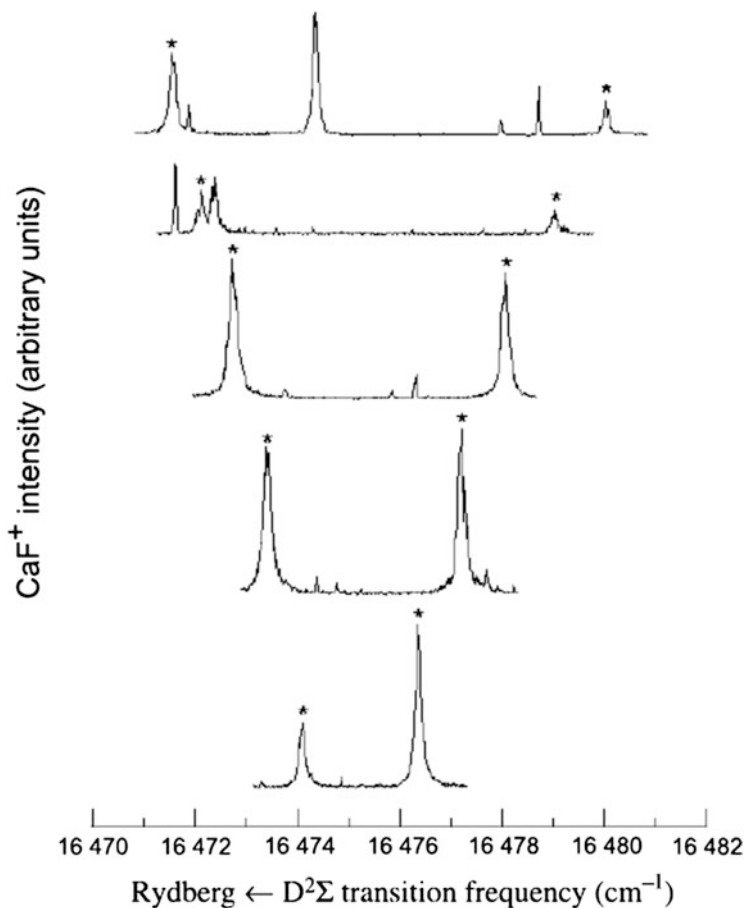


Fig. 2.5 Raw spectrum stacked plot. A consecutive- N' series of optical–optical double resonance spectra of CaF is plotted vs. the frequency of the Rydberg $\leftarrow D^2\Sigma^+$ laser. There is no spectrum-to-spectrum shift to remove the effect of different term value for each intermediate level. This sort of stacked plot reveals the energy level pattern associated with each rotational branch. It is this sort of information that displays the pattern-forming rotational quantum numbers rather than the rigorously conserved rotational quantum numbers. Once a branch pattern is observed, attention is focused on what is the difference between the absolutely known rigorous quantum number and the approximately conserved pattern-forming quantum number. This sort of determination need be done only once for each branch in order to make a plot of the reduced term value, $E^{\text{obs}}(N, \text{parity}) - BN(N + 1)$ vs. N [14]. Reproduced with permission from Fig. 5 in J.J. Kay, D.S. Byun, J.O. Clevenger, V.S. Petrovic, R. Seiler, J.R. Barchi, A.J. Merer, and R.W. Field, *Can. J. Chem.* **82**, 791–803 (2004). Copyright 2004, Canadian Science Publishing or its licensors

To summarize, J is determined by a Term Value Stacked Plot (Fig. 2.4) [14] or by R,P vs Q polarization diagnostics [21]. Then, for the organization of transitions into branches as shown on a Raw Spectrum Stacked Plot (Figs. 2.5 and 2.6), one

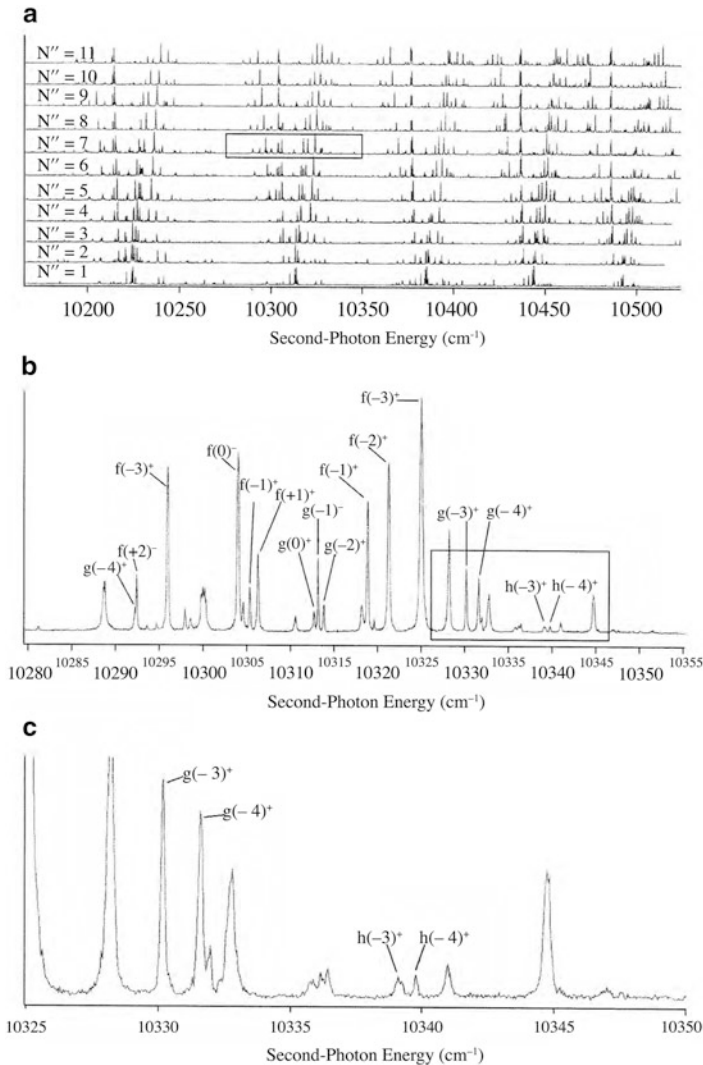


Fig. 2.6 Raw spectrum stacked plot for mostly core-nonpenetrating Rydberg states of CaF. The importance of pattern-forming quantum numbers is illustrated by this three-part figure. The spectral patterns shown in Figs. 2.4 and 2.5 are quite simple, because they involve transitions into core-penetrating Rydberg states. Nonpenetrating states are vastly more numerous and require assignment of *two* nonrigorous but pattern-forming quantum numbers, ℓ and N^+ , where ℓ is the nearly good orbital angular momentum quantum number of the Rydberg electron and N^+ is the nearly good rotational quantum number of the ion-core. It turns out that in CaF the $F'^2\Sigma^+$ intermediate state is prolific in providing transitions to core-nonpenetrating states. Part (a) shows raw stacked plots, from which the observed transitions are organized into many rotational branches. Part (b) shows the detail of the boxed part of the $N'' = 7$ spectrum. Each peak is labeled by its upper state ℓ and $\ell_R = N - N^+$ quantum numbers. ℓ ranges from 3 (f) to 5 (h) and ℓ_R ranges from $+\ell$ to $-\ell$. Part (c) shows even finer detail for the boxed region of the spectrum in part (b) [21]. Reproduced with permission from Fig. 1 in J.J. Kay, S.L. Coy, V.S. Petrovic, B.M. Wong, and R.W. Field, *J. Chem. Phys.* **128**, 194301/1–20 (2008). Copyright 2008, AIP Publishing LLC

uses the reduced term value plot to determine N for at least one transition in each rotational branch. This determines $J - N$ for all of the lines in that branch.

For Rydberg states (Fig. 2.6) at effective principal quantum number $n^* > 10$, rotational branches from transitions into many Rydberg states are closely spaced, perhaps even entangled. OODR is needed to simplify the spectrum and stacked plots make most J and \mathcal{L} (the projection of the orbital angular momentum of the Rydberg electron, ℓ , on the ion-core rotational angular momentum, \mathbf{N}^+ or \mathbf{J}^+) assignments automatic.

2.9 Angular Momenta: A Brief Summary

An angular momentum operator, \mathbf{A} , is *defined* by the commutation rule

$$[\mathbf{A}_i, \mathbf{A}_j] = i\hbar \sum_k \varepsilon_{ijk} \mathbf{A}_k$$

$$\varepsilon_{ijk} = +1 \text{ if } (i, j, k) \rightarrow (x, y, z) \text{ in cyclic order}$$

$$-1 \text{ if } (i, j, k) \rightarrow (x, y, z) \text{ in anticyclic order}$$

$$0 \text{ if one component is repeated}$$

The angular momentum $|A\alpha M_A\rangle$ are simultaneously eigenfunctions of \mathbf{A}^2 , \mathbf{A}_z , and \mathbf{A}_z .

$$\mathbf{A}_z |A\alpha M_A\rangle = \hbar\alpha |A\alpha M_A\rangle$$

$$\mathbf{A}_\pm |A\alpha M_A\rangle = \hbar[A(A+1) - \alpha(\alpha \pm 1)]^{1/2} |A\alpha \pm 1 M_A\rangle^\dagger$$

$$\mathbf{A}_\pm = \mathbf{A}_x \pm i\mathbf{A}_y$$

$$\mathbf{A}^2 |A\alpha M_A\rangle = \hbar^2 A(A+1) |A\alpha M_A\rangle.$$

We are mostly concerned with *body-fixed* angular momentum components (denoted by lower-case x, y, z)

$$(\mathbf{L}, \Lambda), (\mathbf{S}, \Sigma), (\mathbf{J}, \Omega), \quad \mathbf{N} = \mathbf{J} - \mathbf{S}, \mathbf{F} = \mathbf{J} + \mathbf{I}.$$

[†]There is a special complication that arises for the body-fixed components of angular momenta that contain the rotation of the body frame (\mathbf{J} , $\mathbf{N} = \mathbf{J} - \mathbf{S}$, but not \mathbf{L} or \mathbf{S}). For these angular momenta, the body-fixed components follow “reversed angular momentum commutation rules”, $[\mathbf{A}_i, \mathbf{A}_j] = -\sum_k \varepsilon_{ijk} \mathbf{A}_k$, and the roles of \mathbf{A}_+ and \mathbf{A}_- are exchanged.

$$\begin{aligned}\mathbf{L}_z |n\Lambda S\Sigma\rangle &= \hbar\Lambda |n\Lambda S\Sigma\rangle \\ \mathbf{S}_z |n\Lambda S\Sigma\rangle &= \hbar\Sigma |n\Lambda S\Sigma\rangle \\ \mathbf{J}_z |n\Lambda S\Sigma\rangle &= \hbar(\Lambda + \Sigma) |n\Lambda S\Sigma\rangle.\end{aligned}$$

The Stark (electric field) and Zeeman (magnetic field) effects and electronic transition intensities are related to *laboratory*-fixed components of angular momenta (denoted by upper case X, Y, Z)

$$\mathbf{J}_Z |\Omega JM\rangle = \hbar M |\Omega JM\rangle.$$

Just as all of the matrix elements of the magnitude and components of an angular momentum operator, \mathbf{A} , may be derived from the commutation rule definition of \mathbf{A} , other operators, \mathbf{B} , may be classified relative to \mathbf{A} by the commutation rule:

$$[A_i, B_j] = i\hbar \sum_k \epsilon_{ijk} B_k.$$

This reduced form of the Wigner–Eckart Theorem guides evaluation of matrix elements of \mathbf{B} in the $|A\alpha M_A\rangle$ basis set [22].

2.10 Where Have We Been and Where are We Going?

This lecture has been an unconventional introduction to finding the appropriate $\mathbf{H}^{(\text{eff})}$ model. Once we find it, all we need to do is adjust the parameters (molecular constants) that define the $\mathbf{H}^{(\text{eff})}$ to get a good least-squares fit to all of the energy levels. The important trick is to build a simple but physical model that includes all of the terms in the $\mathbf{H}^{(\text{eff})}$ that affect the observed pattern of energy levels and transition intensities. Once we have a spectroscopically well determined $\mathbf{H}^{(\text{eff})}$, we can compute a very large range of spectroscopic and dynamical effects. We have much more than an archival table of molecular constants. This is what I mean by going “beyond the molecular constants”.

References

1. H. Lefebvre-Brion, R.W. Field, *The Spectra and Dynamics of Diatomic Molecules*, Sect. 2.1 (Elsevier, Amsterdam, 2004)
2. R.W. Field, J. Baraban, S.H. Lipoff, A.R. Beck, *Effective Hamiltonians in Handbook of High-Resolution Spectroscopies*, ed. by M. Quack, F. Merkt (Wiley, New York, 2010)
3. H. Lefebvre-Brion, R.W. Field, *The Spectra and Dynamics of Diatomic Molecules*, Sect. 3.2 (Elsevier, Amsterdam, 2004)

4. H. Lefebvre-Brion, R.W. Field, *The Spectra and Dynamics of Diatomic Molecules*, Sect. 3.1 (Elsevier, Amsterdam, 2004)
5. J. von Neumann, E.P. Wigner, *Z. Phys.* **40**, 742 (1927)
6. H. Lefebvre-Brion, R.W. Field, *The Spectra and Dynamics of Diatomic Molecules*, Sect. 5.1.3 (Elsevier, Amsterdam, 2004)
7. R.J. LeRoy, <http://leroy.uwaterloo.ca/programs.html> (RKR1 and LEVEL)
8. J.L. Dunham, *Phys. Rev.* **41**, 721 (1932)
9. Ch.H. Townes, A.L. Schawlow, *Microwave Spectroscopy* (Dover, New York, 2012), pp. 9–13
10. H. Lefebvre-Brion, R.W. Field, *The Spectra and Dynamics of Diatomic Molecules* (Elsevier, Amsterdam, 2004), pp. 181–191
11. H. Lefebvre-Brion, R.W. Field, *The Spectra and Dynamics of Diatomic Molecules* (Elsevier, Amsterdam, 2004), pp. 107–110
12. H. Lefebvre-Brion, R.W. Field, *The Spectra and Dynamics of Diatomic Molecules* (Elsevier, Amsterdam, 2004), p. 100
13. R.W. Field, *Berichte der Bunsengesellschaft für Physikalische Chemie* **86**, 771–779 (1982); C. Linton, M. Dulick, R.W. Field, P. Carette, P.C. Leyland, R.F. Barrow, *J. Mol. Spectrosc.* **102**, 441–497 (1983)
14. J.J. Kay, D.S. Byun, J.O. Clevenger, X. Jiang, V.S. Petrović, R. Seiler, J.R. Barchi, A.J. Merer, R.W. Field, *Can. J. Chem.* **82**, 791–803 (2004)
15. C. Cohen-Tannoudji, B. Diu, F. Laloë, *Quantum Mechanics*, Chap. 11 (Wiley, New York, 1977), pp. 1095–1108
16. H. Lefebvre-Brion, R.W. Field, *The Spectra and Dynamics of Diatomic Molecules* (Elsevier, Amsterdam, 2004), p. 121
17. H. Lefebvre-Brion, R.W. Field, *The Spectra and Dynamics of Diatomic Molecules* (Elsevier, Amsterdam, 2004), p. 131
18. K.C. Cossel, D.N. Gresh, L.C. Sinclair, T. Coffey, L.V. Skripnikov, A.N. Petrov, N.S. Mosyagin, A.V. Titov, R.W. Field, E.R. Meyer, E.A. Cornell, J. Ye, *Chem. Phys. Lett.* **546**, 1–10 (2012)
19. H. Lefebvre-Brion, R.W. Field, *The Spectra and Dynamics of Diatomic Molecules*, Fig. 3.18 (Elsevier, Amsterdam, 2004), p. 215
20. V.S. Petrovic, R.W. Field, *J. Chem. Phys.* **128**, 014301/1–014301/8 (2008)
21. J.J. Kay, S.L. Coy, V.S. Petrović, R.W. Field, *J. Chem. Phys.* **128**, 194301/1–20 (2008)
22. C. Cohen-Tannoudji, B. Liu, F. Laloë, *Quantum Mechanics* (Wiley, New York, 1977), pp. 1049–1055



<http://www.springer.com/978-3-319-15957-7>

Spectra and Dynamics of Small Molecules

Alexander von Humboldt Lectures

Field, R.W.

2015, XII, 153 p. 33 illus., 6 illus. in color., Softcover

ISBN: 978-3-319-15957-7